

# Unconventional Zigzag Indium Phosphide Single-Crystalline and Twinned Nanowires

Guozhen Shen,\* Yoshio Bando, Baodan Liu, Chengchun Tang, and Dmitri Golberg

Nanoscale Materials Center, National Institute for Materials Science, Namiki 1-1, Tsukuba, Ibaraki 305-0044, Japan

Received: December 14, 2005; In Final Form: June 5, 2006

Unconventional zigzag indium phosphide (InP) single-crystalline and twinned nanowires were produced via thermal evaporation of indium phosphide in the presence of zinc selenide. The structure and morphology of the as-synthesized products were characterized by X-ray diffraction, scanning electron microscopy, and transmission electron microscopy. Studies found that two type of nanowires exist in the products, namely, the periodic-rhombus-decorated single-crystalline InP (type I) nanowires and jagged twinned InP (type II) nanowires. Both of them have preferential  $\langle 111 \rangle$  growth directions. The optical properties were also investigated at room temperature, and they show that the nanowires display a strong emission at  $\sim 750$  nm, which is quite different from that observed in all previous reports related to the InP nanostructures.

## Introduction

One-dimensional (1D) nanomaterials in the form of tubes, wires, and belts have attracted significant attention over the past decade because of their interesting geometries, novel properties, and potential applications in many fields.<sup>1–3</sup> For non-carbon-based 1D nanostructures, real devices have been fabricated through utilizing semiconductor nanowires made of Si, InP, etc.<sup>4</sup> Among several kinds of 1D nanostructures, the zigzag-shaped 1D structures represent an unusual group of nanomaterials, which process an additional geometry-driven property tenability within the building blocks of nanoscale devices.<sup>5</sup> Several kinds of 1D zigzag nanostructures including  $\text{Ga}_2\text{O}_3$ , AlN,  $\text{Al}_2\text{O}_3$ , GaN, PbSe, etc. have already been synthesized.<sup>5</sup>

As an important semiconductor among the group IIIA phosphide semiconductors, nanoscale-sized indium phosphide (InP) has attracted prime interest for nanostructure research because of its potential applications in fiber optical communications, high-speed electronic devices, optoelectronics, etc. To date, several kinds of methods have been adopted for the synthesis of one-dimensional InP nanostructures, for example, nanowires and nanotubes. For example, Lieber and co-workers<sup>6</sup> synthesized single-crystalline InP nanowires by a laser-assisted catalytic growth (LCG). Buhro and co-workers<sup>7</sup> have pioneered the solution-liquid–solid (SLS) model for the InP nanowire synthesis. Xie and co-workers<sup>8</sup> successfully synthesized InP nanowires in a surfactant-assisted aqueous solution. Banin and co-workers<sup>9</sup> synthesized InP nanorods from the reaction between tris(trimethylsilyl) phosphine  $[(\text{TMS})_3\text{P}]$  and  $\text{InCl}_3$  in trioctylphosphine oxide (TOPO) with gold nanoparticles as catalysts. A metal–organic vapor-phase epitaxial method was also developed to synthesize InP nanowires by Bhunia et al.<sup>10</sup> Crystalline InP nanotubes were also fabricated by the VLS laser ablation method.<sup>11</sup> Very recently, our group has successfully synthesized InP nanowires and nanotubes by simple thermal chemical routes without templates.<sup>12</sup>

In this paper, we report on the synthesis of unconventional zigzag-shaped InP single-crystalline nanowires and twinned nan-

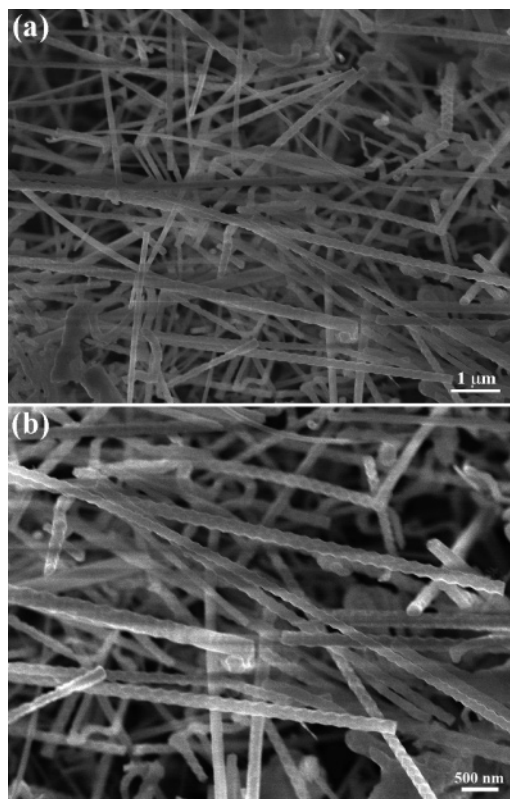


Figure 1. SEM images of the as-grown InP product.

owires via a simple thermal evaporation route without the use of any catalyst or templates; instead a ZnSe synthesis promoter is used. The structures, morphologies, and optical properties of the nanowires are studied. The nanowires display a strong emission at  $\sim 750$  nm, which is quite different from that observed in all previous reports related to the InP nanostructures.

## Experimental Procedures

Zigzag InP single-crystalline nanowires and twinned nanowires were synthesized in a vertical induction furnace consisting of a fused quartz tube and an induction-heated cylinder made

\* Corresponding author: e-mail SHEN.Guozhen@nims.go.jp; fax +81-29-851-6280.

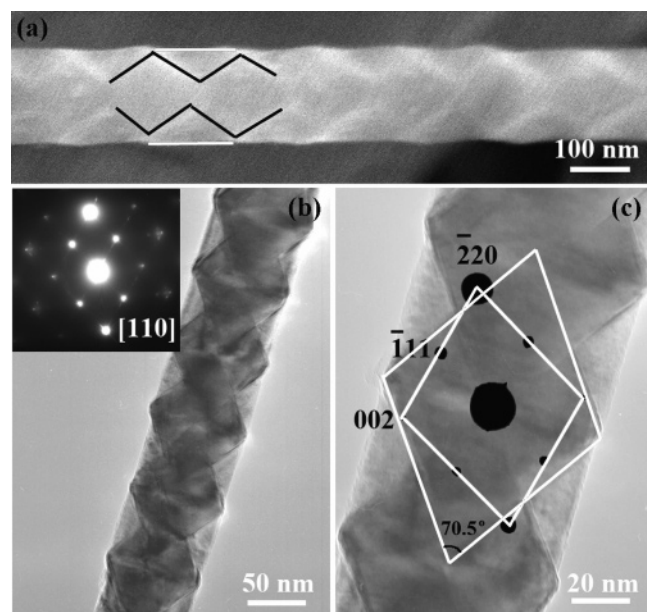


**Figure 2.** (a) SEM image and (b, c) TEM images of a periodic-rhombus-decorated single-crystalline InP nanowire.

of high-purity graphite coated with a C fiber thermoinsulating layer. The furnace had inlet and outlet C pipes on its base. A graphite crucible containing InP (0.8 g) and ZnSe (0.1 g) was placed at the center cylinder zone. Before heating, the quartz tube was evacuated to  $\sim 0.2$  Torr to eliminate  $O_2$ . Then a pure Ar flow was set within the carbon cylinder at a constant rate of 250 sccm and at the ambient pressure in the tube. The furnace was rapidly heated and kept at 1200  $^{\circ}\text{C}$  for 1 h.

After the reaction was terminated and the furnace cooled to room temperature, the collected products were characterized by scanning electron microscopy (SEM, JSM-6700F) and by use of a transmission electron microscope (HRTEM, JEM-3000F) equipped with an X-ray energy dispersive spectrometer (EDS). Photoluminescence spectra were collected at room temperature with a He–Cd laser line at 325 nm as the excitation source.

## Results and Discussion

After the reaction, a large quantity of a black-colored product was deposited on the inner wall of a graphite crucible. Scanning electron microscopy (SEM) observation reveals the general morphology of the product (Figure 1). It shows wiggly wirelike nanostructures. Each wiggly nanowire has a diameter of ca. 100

nm and a length of several tens of micrometers. Energy-dispersive X-ray spectrometry (EDS) reveals that the product consists of In and P elements at an atomic ratio close to the InP stoichiometry. Closer examination by high-magnified SEM and transmission electron microscopy (TEM) shows that there exist two types of 1D InP nanostructures: periodic-rhombus-decorated single-crystalline InP (type I) nanowires and jagged twinned InP (type II) nanowires.

Figure 2a depicts the high-magnification SEM image of a typical periodic-rhombus-decorated single-crystalline InP nanowire with a diameter of  $\sim 120$  nm. It can be seen that this kind of nanowire is characterized by a complex highly symmetrical structure. On each type I nanowire, many rhombuses are connected with each other along the longitudinal axis of the nanowire. Further characterization by TEM analysis also confirms this periodic-rhombus-decorated complex structure as shown in Figure 2b. The corresponding selected area electron diffraction (SAED) pattern (Figure 2b, inset) verifies the single crystalline nature of the type I nanowire. The spots on the pattern can be attributed to the  $[110]$  zone axis of a cubic InP crystal. Figure 2c illustrates the overlay of an image of a single rhombus and its SAED pattern. The inside rhombus angles, as indicated in this image, is  $70.5^{\circ}$ , in accordance with the standard value.

Detailed structural analysis of the type I nanowires was carried further by high-resolution TEM (HRTEM). Figure 3a clearly displays two rhombuses in a single type I nanowire. The angle of a rhombus corner marked in Figure 3b is  $\sim 109.5^{\circ}$ , in agreement with the angle between two  $(111)$  planes in an InP crystal. EDS generated with an electron nanoprobe ( $\sim 20$  nm) was used to check the composition of the nanowires and the spectrum is shown in Figure 3b. It shows the presence of In and P elements, indicating the formation of InP. Trace Zn and Se were also detected in this figure, showing the incorporation of Zn and Se into the InP nanowires. Figure 3d,e depicts the HRTEM images of the area framed in Figure 3c. The clearly resolved fringes with 0.3 nm separation in Figure 3d are typical for the  $(200)$  plane  $d$  spacing in cubic InP. The  $d$  spacing of 0.21 nm in Figure 3e corresponds to the  $(220)$  plane separation of cubic InP. On the basis of the SAED pattern and HRTEM images, it can be suggested that the type I nanowires are single crystals with the preferential growth direction along the  $\langle 111 \rangle$  orientation, as marked in Figure 3d,e.

The SEM image of a typical jagged twinned InP (type II) nanowire is presented in Figure 4a. In general, the type II nanowires have diameters of 90–150 nm within pseudoperiodic zigzag structures. The TEM image of a single nanowire in Figure

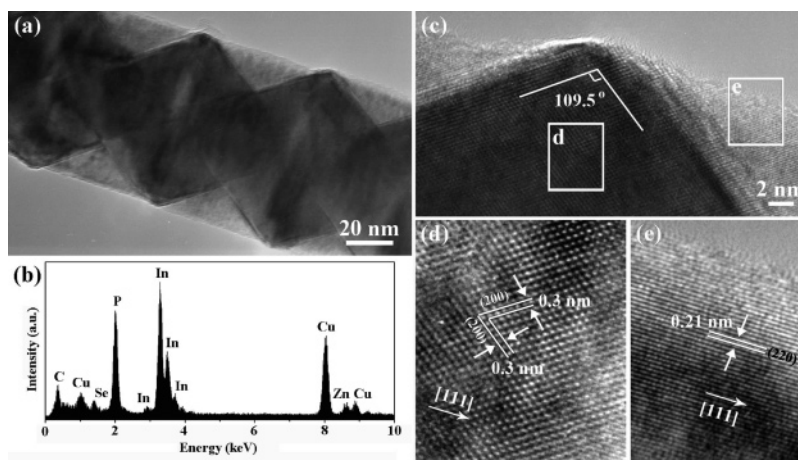


**Figure 3.** (a) Low-magnification TEM image and (b) EDS spectrum of a periodic-rhombus-decorated single-crystalline InP nanowire. (c) HRTEM image of the corner of a single rhombus. (d, e) Lattice-resolved TEM images of the parts framed in panel c.



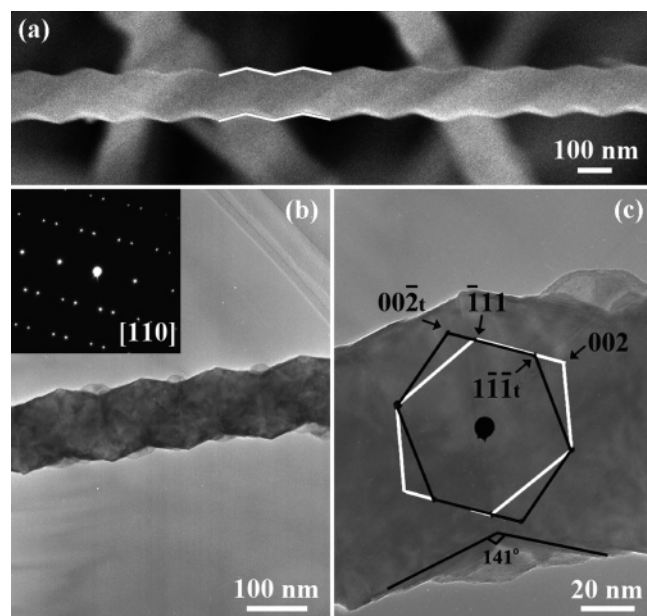


**Figure 4.** (a) SEM image and (b, c) TEM images of a jagged twinned InP nanowire.

4b also confirms that the nanowire is composed of periodic twins along its entire length and width with a corresponding twinning period close to  $\sim 50$  nm. The zone axis of the corresponding SAED pattern in the inset is also along the  $[110]$  direction of the cubic InP. Twin faults are clearly visible in the SAED pattern (Figure 4b,c). Here, the “twin” reflections are indexed with a subscript  $t$  and the remaining matrix reflections are indexed without subscript. It is well-known that the  $(111)$  twinned crystals have a relative rotational angle of  $70.5^\circ$ . Therefore, the inside zigzag angles, as indicated in Figure 4c, can be given as  $141^\circ$ , in accordance with the theoretical estimation.

Further structural analysis of the type II nanowires was also performed by HRTEM (Figure 5). Figure 5a is the TEM image of a typical type II nanowire. Its EDS spectrum, shown in Figure 5b, also confirms the formation of InP with the incorporation of trace Zn and Se. Figure 5c is the TEM image of the joint corner marked in Figure 5a. The twin boundaries of the type II nanowire are clearly seen, as marked within the circle in Figure 5c. It shows that the boundaries are rich in defects, in accordance with previous reports on twinned nanowires.<sup>13</sup> Figure 5d,e demonstrates the lattice-resolved HRTEM images of the framed

parts in Figure 5c. The  $d$  spacings of 0.3 nm in both images correspond well to the  $(200)$  lattice spacing of cubic InP. The SAED pattern and HRTEM images analyses indicate that the type II nanowires also have the same preferential  $\langle 111 \rangle$  growth direction as that of the type I nanowires. According to the TEM and SAED results, the adjacent twin blocks can be shown in Figure 6, which can be explained by rotating  $180^\circ$  with respect to each other with a rotational axis of  $\langle 111 \rangle$ .

In the present synthetic runs no metal catalysts are used. No particles attached to the nanowires were found, implying that the formation of the present nanostructures is presumably governed by the vapor–solid (VS) mechanism. Importantly, the usage of a ZnSe synthesis promoter is undoubtedly the key factor for the preparation of unconventional InP nanowires, though it is yet unclear what exact influence ZnSe has had. It is emphasized here that without the ZnSe utilization, only standard straight and smooth single crystalline InP nanowires were obtained. A previous report by Bakkers and Verheijen<sup>11</sup> about the laser ablation synthesis of InP nanotubes had suggested that the morphology of the InP nanotubes depended on the dopants added to the InP targets. At high reaction temperature, both InP and ZnSe are evaporated and transferred to the low-temperature region. The existence of ZnSe vapors greatly varies the vapor pressure and concentration of InP vapors. In fact, for the growth of nanostructures, the gradient in the source material concentration around the growing surface is essential for the crystal morphology of nanomaterials.<sup>14</sup> Thus the existence of ZnSe is very important to the growth of zigzag InP nanostructures as proved by our experiments. The present unique nanostructures confirm their suggestions, and the morphology of the zigzag InP nanowires is likely determined by the specific growth kinetics. Both the single crystalline and twinned nanowires may somehow form during the nucleation and growth processes.<sup>15</sup> For example, phase transformation, crystal growth from the different phases, or recrystallization of the solid phase should be taken into account. The synthesis of zigzag InP nanostructures was performed in a vertical induction furnace, which provides more rapid temperature change than the conventional tube furnace. Rapid temperature change during the nucleation and growth processes and the existence of ZnSe vapors, as well as the nanosized structures, lead to the generation of high internal stress in InP structures. Shear strain is then invoked to release the stress, which resulted in the formation of twin crystal nanostructures or rhombus-decorated nanostructures.

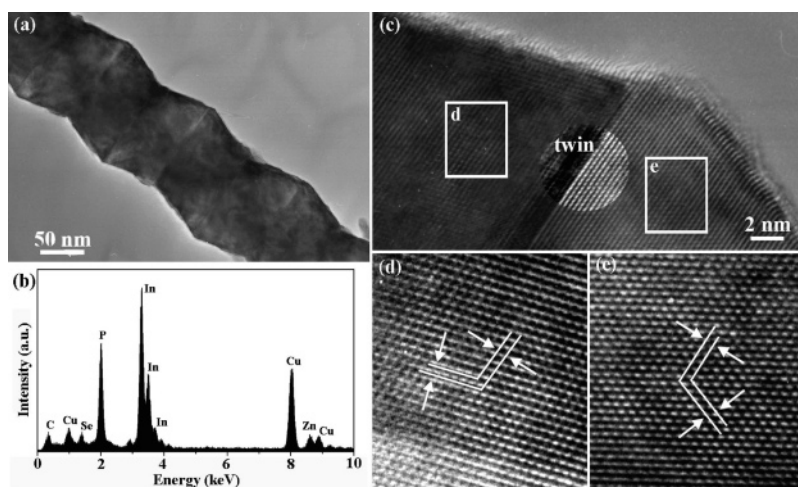


**Figure 5.** (a) Low-magnified TEM image of a jagged twinned InP nanowire. (b) HRTEM image of the part framed in panel a. (c, d) Lattice-resolved TEM images of the parts framed in panel b.

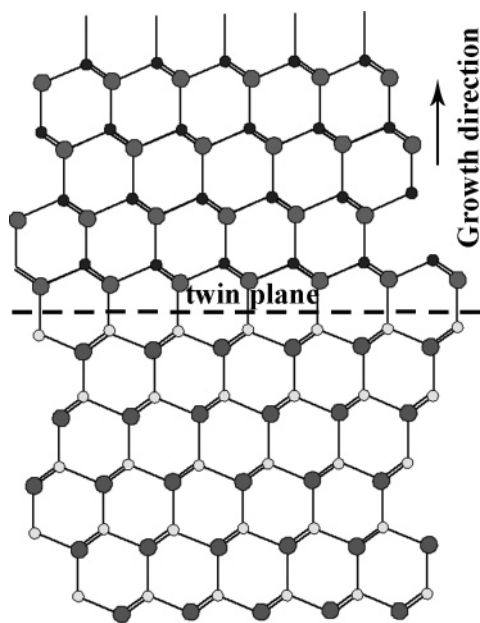


**Figure 6.** Illustration of the type II twinned nanowires showing the two adjacent rotational twin domains.

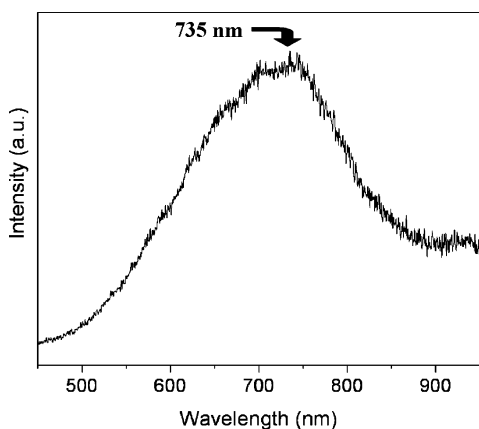


**Figure 7.** Room-temperature PL spectra of the zigzag InP nanowires.

The room-temperature photoluminescence (PL) spectra of the as-synthesized InP nanowires were finally measured (Figure 7). The representative spectrum exhibits a strong emission peak at 735 nm (about 1.69 eV). Previous reports have shown that conventional InP nanowires usually emit in the range of 800–900 nm.<sup>6,11</sup> Bakkers and Verheijen<sup>11</sup> reported that the InP nanotubes with diameter of 27 nm have emission at 590 nm due to the quantum confinement effect. However, the quantum confinement effect cannot be used to explain the present emission at 735 nm since the present unconventional InP nanostructures have relatively large diameters of ca. 100 nm, largely exceeding the exciton Bohr radius of ~20 nm. Recently, van Vugt et al.<sup>16</sup> systematically investigated the PL properties of InP nanowires. The InP nanowires can be passivated by a photoetching process to increase the luminescence efficiency considerably. A blue or red shift of the exciton energy can occur, depending on the effective masses of the electron and hole in the nanostructures. Furthermore, some other works have showed that with the incorporation of proper dopants, new PL peaks may be induced for a given nanowire.<sup>17</sup> On the basis of the above reports, we assume that the novel peak at 735 nm can be

explained in a similar way. EDS analysis has shown that both Zn and Se are incorporated in the zigzag InP nanowires. These dopants may introduce a high density of defects in the nanowires. Since a single defect site can strongly affect the PL properties of a single nanowire, PL emission can be greatly shifted and the peak at 735 nm thus appeared.

## Conclusions

In summary, unconventional zigzag InP single-crystalline nanowires and twinned nanowires were synthesized via thermal evaporation of indium phosphide in the presence of zinc selenide. Both the periodic-rhombus-decorated single-crystalline InP (type I) nanowires and jagged twinned InP (type II) nanowires have preferential  $\langle 111 \rangle$  growth directions. Compared with the conventional InP nanowires with smooth surfaces and uniform diameters, the unusual zigzag InP nanowires exhibit unique structural characteristics and novel optical properties, which may find applications in optoelectronic devices.

## References and Notes

- (1) (a) Iijima, S. *Nature* **1991**, *354*, 56. (b) Morales, A.; Lieber, C. M. *Science* **1998**, *279*, 208. (c) Pan, Z. W.; Dai, Z. R.; Wang, Z. L. *Science* **2001**, *291*, 1947. (d) Hu, J. Q.; Bando, Y.; Liu, Z. W.; Zhan, J. H.; Golberg, D.; Sekiguchi, T. *Angew. Chem., Int. Ed.* **2004**, *43*, 63.
- (2) (a) Nath, M.; Govindaraj, A.; Rao, C. N. R. *Adv. Mater.* **2001**, *13*, 283. (b) Goldberger, J.; He, R.; Zhang, Y.; Lee, S.; Yan, H.; Choi, H.; Yang, P. D. *Nature* **2003**, *422*, 599.
- (3) (a) Xia, Y. N.; Yang, P. D.; Sun, Y.; Wu, Y.; Mayers, B.; Gates, B.; Yin, Y.; Kim, F.; Yan, H. *Adv. Mater.* **2003**, *15*, 353. (b) Dai, H. J. *Acc. Chem. Res.* **2002**, *35*, 1035. (c) Patzke, G. R.; Krumeich, F.; Nesper, R. *Angew. Chem., Int. Ed.* **2002**, *41*, 2446. (d) Zhang, R. Q.; Lifshitz, Y.; Lee, S. T. *Adv. Mater.* **2003**, *15*, 635.
- (4) (a) Lieber, C. M. *Science* **2001**, *291*, 851. (b) Chen, D.; Tang, K. B.; Liang, Z. H.; Liu, Y. K.; Zheng, H. G. *Nanotechnology* **2005**, *16*, 2619. (c) Huang, Y.; Duan, X. F.; Cui, Y.; Lauhon, L.; Kim, K.; Lieber, C. M. *Science* **2001**, *294*, 1313. (d) Liu, B. Y.; Wei, L. W.; Ding, Q. M.; Yao, J. L. *Nanotechnology*, **2004**, *15*, 1745.
- (5) See for example (a) Zhan, J. H.; Bando, Y.; Hu, J. Q.; Xu, F. F.; Golberg, D. *Small* **2005**, *1*, 883. (b) Cho, K. S.; Talapin, D. V.; Gaschler, W.; Murray, C. B. *J. Am. Chem. Soc.* **2005**, *127*, 7140. (c) Duan, J. H.; Yang, S. G.; Liu, H. W.; Gong, J. F.; Huang, H. B.; Zhao, X. N.; Zhang, R.; Du, Y. W. *J. Phys. Chem. B* **2005**, *109*, 3701.
- (6) (a) Duan, X. F.; Huang, Y.; Cui, Y.; Wang, J. F.; Lieber, C. M. *Nature* **2001**, *409*, 66. (b) Wang, J. F.; Gudiksen, M. S.; Duan, X. F.; Cui, Y.; Lieber, C. M. *Science* **2001**, *293*, 1455. (c) Duan, X. F.; Lieber, C. M. *Adv. Mater.* **2000**, *12*, 298.
- (7) Trentler, T. J.; Hickman, K. M.; Goel, S. C.; Viano, A. M.; Gibbons, P. C.; Buhro, W. E. *Science* **1995**, *270*, 1791.
- (8) Xiong, Y.; Xie, Y.; Li, Z.; Li, X.; Gao, S. *Chem.—Eur. J.* **2004**, *10*, 654.
- (9) Kan, S.; Mokari, T.; Rothenberg, E.; Banin, U. *Nat. Mater.* **2003**, *2*, 155.
- (10) Bhunia, S.; Kawamura, T.; Watanabe, Y.; Fujikawa, S.; Tokushima, K. *Appl. Phys. Lett.* **2003**, *83*, 3371.
- (11) Bakkers, E. P. A. M.; Verheijen, M. A. *J. Am. Chem. Soc.* **2003**, *125*, 3440.
- (12) (a) Tang, C. C.; Bando, Y.; Liu, Z. W.; Golberg, D. *Chem. Phys. Lett.* **2003**, *376*, 676. (b) Yin, L. W.; Bando, Y.; Golberg, D.; Li, M. S. *Appl. Phys. Lett.* **2004**, *85*, 3869.
- (13) (a) Chen, H.; Wang, J.; Yu, H.; Yang, H.; Xie, S. S.; Li, J. *J. Phys. Chem. B* **2005**, *109*, 2573. (b) Fang, X. S.; Ye, C. H.; Zhang, L. D.; Xie, T. *Adv. Mater.* **2005**, *17*, 1661.
- (14) (a) Imai, H.; Oaki, Y. *Angew. Chem., Int. Ed.* **2004**, *43*, 1363. (b) Shen, G. Z.; Bando, Y.; Liu, B. D.; Golberg, D.; Lee, C. J. *Adv. Funct. Mater.* **2006**, *16*, 410.
- (15) (a) Christian, J. W.; Mahajan, S. *Prog. Mater. Sci.* **1995**, *39*, 1. (b) Wang, Z. L.; Dai, Z. R.; Gao, R. P.; Bai, Z. G.; Golberg, J. L. *Appl. Phys. Lett.* **2000**, *77*, 3349.
- (16) Van Vugt, L. K.; Veen, S. J.; Bakkers, E. P. A. M.; Roest, A. L.; Vanmaekelbergh, D. *J. Am. Chem. Soc.* **2005**, *127*, 12357.
- (17) (a) Hu, J. Q.; Bando, Y.; Liu, Z. W. *Adv. Mater.* **2003**, *15*, 1000. (b) Chang, P. C.; Fan, Z.; Tseng, W. Y.; Rajagopal, A.; Liu, J. G. *Appl. Phys. Lett.* **2005**, *87*, 222102.